doi:10.1093/brain/awr054 Brain 2011: 134; 1277–1292 | 1277

BRAIN
A JOURNAL OF NEUROLOGY

Human neuropathological and animal model evidence supporting a role for Fas-mediated apoptosis and inflammation in cervical spondylotic myelopathy

Wen Ru Yu,[1] Tianyi Liu,[1] Tim-Rasmus Kiehl[2,3] and Michael G. Fehlings[1,4,5,6]

1 Division of Genetics and Development, Toronto Western Research Institute, Krembil Neuroscience Centre, Toronto Western Hospital, University Health Network, Toronto, M5T 2S8, Canada
2 Department of Pathology, Toronto Western Research Institute, Krembil Neuroscience Centre, Toronto Western Hospital, University Health Network, Toronto, M5T 2S8, Canada
3 Laboratory Medicine and Pathobiology, Neuroscience Program, University of Toronto, M56 1A8, Canada
4 Division of Neurosurgery, Toronto Western Research Institute, Krembil Neuroscience Centre, Toronto Western Hospital, University Health Network, Toronto, M5T 2S8, Canada
5 Department of Surgery, Krembil Neuroscience Centre, Toronto Western Hospital, University Health Network, Toronto, M5T 2S8, Canada
6 Department of Surgery, Institute of Medical Science, University of Toronto, Toronto, M56 1A8, Canada

Correspondence to: Michael G. Fehlings, MD, PhD, FRCSC,
Krembil Chair in Neural Repair and Regeneration,
The Toronto Western Hospital,
University Health Network,
Room 4W-449,
399 Bathurst Street,
Toronto, Ontario M5T 2S8,
Canada
E-mail: michael.fehlings@uhn.on.ca

Although cervical spondylotic myelopathy is a common cause of chronic spinal cord dysfunction in humans, little is known about the molecular mechanisms underlying the progressive neural degeneration characterized by this condition. Based on animal models of cervical spondylotic myelopathy and traumatic spinal cord injury, we hypothesized that Fas-mediated apoptosis and inflammation may play an important role in the pathobiology of human cervical spondylotic myelopathy. We further hypothesized that neutralization of the Fas ligand using a function-blocking antibody would reduce cell death, attenuate inflammation, promote axonal repair and enhance functional neurological outcomes in animal models of cervical spondylotic myelopathy. We examined molecular changes in post-mortem human spinal cord tissue from eight patients with cervical spondylotic myelopathy and four control cases. Complementary studies were conducted using a mouse model of cervical spondylotic myelopathy (twy/twy mice that develop spontaneous cord compression at C2–C3). We observed Fas-mediated apoptosis of neurons and oligodendrocytes and an increase in inflammatory cells in the compressed spinal cords of patients with cervical spondylotic myelopathy. Furthermore, neutralization of Fas ligand with a function-blocking antibody in twy/twy mice reduced neural inflammation at the lesion mediated by macrophages and activated microglia, glial scar formation and caspase-9 activation. It was also associated with increased expression of Bcl-2 and promoted dramatic functional neurological recovery. Our data demonstrate, for the first time in humans, the potential contribution of Fas-mediated cell death and inflammation to the pathobiology of cervical spondylotic myelopathy. Complementary data in a murine model of cervical spondylotic myelopathy further suggest that targeting the Fas death receptor pathway is a viable neuroprotective strategy to attenuate neural

Received September 14, 2010. Revised February 3, 2011. Accepted February 4, 2011. Advance Access publication April 13, 2011

degeneration and optimize neurological recovery in cervical spondylotic myelopathy. Our findings highlight the possibility of medical treatments for cervical spondylotic myelopathy that are complementary to surgical decompression.

Keywords: cervical spondylotic myelopathy; Fas-mediated apoptosis; inflammation

Abbreviations: CSM = cervical spondylotic myelopathy; GFAP = glial fibrillary acidic protein; TUNEL = terminal deoxynucleotidyl transferase dUTP nick end labelling

Introduction

Cervical spondylotic myelopathy (CSM) is the most common cause of spinal cord impairment in industrialized countries and is characterized by spinal cord compression due to spondylosis, degenerative disc disease or ossification of the posterior longitudinal ligament (Bohlman and Emery, 1988; Swagerty, 1994; McCormack and Weinstein, 1996; Fehlings and Skaf, 1998). The principal neuropathological features of CSM include cystic cavitation, gliosis, Wallerian degeneration of descending and ascending fibre tracts, and anterior horn cell loss (Bohlman and Emery, 1988; Swagerty, 1994; McCormack and Weinstein, 1996; Ohwada *et al*., 1996; Fehlings and Skaf, 1998). Clinically, CSM is associated with signs of spinal cord impairment including gait disturbance, clumsiness and paraesthesia of the hands, along with signs of pyramidal and posterior column dysfunction (Nakamura *et al*., 1999). In contrast, there is limited understanding of the biochemical and molecular mechanisms underlying the progressive neural degeneration in this condition. Despite advances in the surgical treatment for CSM, many, if not most, patients are left with substantial neurological disability related to underlying permanent structural injury to the spinal cord. Hence, the development of neuroprotective strategies that could be used as a complementary approach to surgical decompression for CSM would be of great clinical importance.

Increasing evidence in models of neurotrauma and neurodegeneration has demonstrated that Fas, a receptor known to be involved in cell death mechanisms, plays an important role in mediating neural apoptosis and provoking an inflammatory response through the release of proinflammatory cytokines (Felderhoff-Mueser *et al*., 2000; Desbarats *et al*., 2003; Demjen *et al*., 2004; Casha *et al*., 2005). Genetic Fas deficiency (Yoshino *et al*., 2004; Casha *et al*., 2005; Yu *et al*., 2009*b*), competitive inhibition of Fas activation with a CD95-Fc reagent (Ackery *et al*., 2006) or neutralization of Fas ligand with an anti-Fas ligand antibody markedly reduces death of neurons and oligodendrocytes and improves functional recovery of spinal injured animals and stroke (Martin-Villalba *et al*., 2001; Demjen *et al*., 2004; Ackery *et al*., 2006; Yu *et al*., 2009*b*). Neutralization of CD95L also reduces the initial infiltration of inflammatory cells, creating an inflammatory response that facilitates recovery of locomotor function after spinal cord injury (Letellier *et al*., 2010). Neutralization of Fas ligand in traumatically injured wild-type spinal cord cultures reduced the expression of truncated BID and activation of caspase-9 (Yu *et al*., 2009*a*). Moreover, recent results from our laboratory have demonstrated a role for Fas-mediated apoptosis of neurons and oligodendrocytes in twy/twy mice, which develop spontaneous ossification of the ligamentum flavum at C2–C3, followed by progressive cord compression (Yu *et al*., 2009*a*). Based on promising results and previous work in models of traumatic spinal cord injury, we hypothesize that Fas-mediated apoptosis and inflammation play a role in spinal cord degeneration in human CSM and in twy/twy mice. In the present study, we provide for the first time, evidence that Fas-mediated apoptosis and inflammation plays a prominent role in the pathobiology of human CSM. We also, for the first time, demonstrate that neutralization of Fas ligand with a function-blocking antibody reduces cell death and inflammation and dramatically enhances functional neurological outcomes in twy/twy mice. Our data strongly suggest that the Fas receptor could be an attractive clinical therapeutic target to attenuate neural degeneration in CSM, a potential complementary treatment to surgical decompression.

Materials and methods

Clinical data for human cervical spondylotic myelopathy

The clinical and pathological data are summarized in Table 1. The principal causes of death in six patients with CSM were secondary to cardiorespiratory complications occurring within 3–10 days of surgery. One patient died from mesenteric infarction and bowel obstruction and one patient died as a result of cerebral infarction; both 6 weeks postoperatively. The causes of mortality for four control patients (2 male, 2 female: mean age 69.5 ± 6.7, range 56–85) were due to conditions unrelated to the CNS. The patients ranged from 61 to 89 years of age (6 male, 2 female: mean age 73 ± 9.7) and the time from CSM onset to death ranged from 6 months to 50 years. Motor weakness of the upper or lower extremities with spastic paraparesis and gait disturbance was seen in six patients. Sensory disturbances were observed in five patients. Hyper-reflexia of deep tendon stretch reflexes was exaggerated in four patients. CT/myelography or MRI showed multilevel spondylotic changes, with narrowing of spinal canal and cord compression in all patients with CSM.

Morphological methods

In all cases with CSM but one, autopsies were performed between 1 and 24 h after death. In the remaining case, the autopsy was conducted at 30 h post-mortem. Spinal cords were removed and fixed in 10% neutral buffered formalin. The uninjured caudal sections served as a within-case control. Sections from four non-patients with CSM were used as normal controls. Sections of paraffin tissue, cut at 5 μm thickness and placed on positively charged glass slides, were

Table 1 Summary of the clinical features from the human CSM and control cases

Case	Age	Sex	Years of disease	Level	History of CSM or other significant disorder	Pathological findings in spinal cord	Causes of death	Post-mortem
1	89	F	11	C3-8	Numbness of hand and fingers for 3 months, slight spastic paraparesis. Weakness of right elbow flexors. Eleven years post-cervical laminectomy	Patchy, focal areas of degeneration with demyelination involved corticospinal tract and dorsal roots; degeneration involving ascending posterior columns; gliosis and C5-8 anterior horn cell loss	Mesenteric infarction with bowel obstruction	1 day
2	61	M	8	C3-6	Marked paraesthesiae and weakness in the upper limbs, with impaired balance CT confirmed spondylitic disease at two levels with ventral compression	Gliosis with cystic cavitation of central grey matter and posterior columns; moderate anterior horn cell loss; degeneration of lateral and posterior columns, dorsal roots and dorsal root entry zone	Four days post-anterior decompression and fusion: acute myocardial infarction	1 day
3	75	F	>5	C3-6	Gait ataxia treated by laminectomy 10 years previously	Focal degenerative lesions in lateral and anterior columns	Pneumonia	1 day
4	83	M	0.5	C3-4	Progressive spastic paraparesis; no surgery	Section showed demyelination and gliosis of the lateral columns	CVA; pituitary infarction	1 day
5	66	M	3–4	C5-T1	Progressive four limb numbness and weakness (R > L); severe posterior column dysfunction	Marked anterolateral compression and degeneration and demyelination of corticospinal tracts, posterior and dorsal columns, focal in C5-T1; schwannosis; severe anterior horn cell loss	Four days post-laminectomy: acute myocardial infarction	12 h
6	73	M	4	C4-6	Progressive dysaesthesia and stiffness in the shoulders, arms and legs; gait ataxia; diffuse limb hyper-reflexia CT myelogram: significant C4-6 compression associated with cervical spondylosis osteophyte formation	Severe loss of myelinated axons in posterior and lateral columns; loss of motoneurons; spongy degeneration of neuropil	One day post-anterior decompression and fusion: pulmonary oedema and cardiac arrest	6 h
7	63	M	10	C2-7	Progressive gait difficulties and tetraparesis; dorsal column dysfunction; CT: cervical cord compression with severe spondylosis and ossification of posterior longitudinal ligament	Degeneration of the posterior columns and corticospinal tracts; moderate ventral horn cell loss	Six weeks post-anterior decompression and fusion: respiratory compromise and subsequent cardiorespiratory arrest	1 h
8	74	M	50	C5-T2	Progressive spastic paraparesis 5 years; wasting and weakness of left hand intrinsics; hyperreflexia of lower limbs; upgoing plantar responses X-ray: C3-T1 obliteration of disc spaces and massive osteophyte formation	Severe anterior horn neuronal loss and gliosis in C7-T1; ascending and descending Wallerian degeneration	Three days post-anterior decompression and fusion: cardiac arrest	1 day
9	56	M	–	–	Guillain–Barre syndrome Type I diabetes mellitus	NIL	Respiratory failure	12 h
10	61	F	–	–	Vestibular schwannoma	NIL	Right transverse sinus thrombosis post-resection of right vestibular schwannoma	30 h
11	76	F	–	–	NIDDM, atrial fibrillation, congestive cardiac failure	NIL	Congestive cardiac failure/arrest	8 h
12	85	M	–	–	Dementia, pleural effusion, atherosclerosis, peptic ulcer, prostatomegaly, nephrosclerosis	NIL	Respiratory failure	12 h

CVA = cerebrovascular accident; L = left; NIDDM = non-insulin-dependent diabetes mellitus; R = right.

retrieved from the tissue archive of the Pathology Department, University Health Network, Toronto, Canada. Two tissue sections per case, taken from both the epicentre of compression and the uninjured caudal region were used for morphological assessment with haematoxylin and eosin, and Luxol fast blue. The remaining sections were used for immunohistochemistry.

Immunohistochemical analysis for human cervical spondylotic myelopathy

After deparaffinization in xylene and rehydration through a series of graded ethyl alcohols for human sections, sections from the epicentre of compression and from caudal regions of CSM and control cases were treated by microwaving in 10 mM citrate buffer pH 6.0 for 10 min and rinsed three times for 5 min in phosphate-buffered saline. Endogenous peroxidase from deparaffinized sections from human CSM was inactivated by treatment with 0.3% H_2O_2 in phosphate-buffered saline for 30 min. Sections were blocked with 1% bovine serum albumin and 5% non-fat milk with 0.3% Triton X-100 for 1 h. Slides were incubated in blocking solution overnight at 4°C with the following primary antibodies: rabbit anti-Fas and anti-Fas ligand (1:100; Santa Cruz Biotechnology), anti-β-amyloid precursor protein (β-APP; 1:4000, Chemicon International Inc) to label damaged axons; anti-PG-M1 (CD68: 1:50, Dako), directed against CD68, a lysosomal protein expressed by phagocytic macrophages of microglial and monocytic origin; anti-ionized calcium binding adaptor molecule 1 (Iba1), expressed in both ramified and activated microglia (polyclonal, 1:300 Wako Pure Chemical Industries); anti-CD3 (1:200, Dako) recognizing human mature T lymphocytes; and anti-myeloperoxidase (MPO; 1:50, Dako), a marker of all neutrophils, and matrix metalloproteinase-9 (MMP-9; 1:100, Chemicon), a proinflammatory protease, activated caspase-3 (1:200, Cell Signaling Technology), activated caspase-7 and -9 (1:150 and 1:1500 Nov Littleton, respectively). Following extensive rinsing in 0.1 M phosphate-buffered saline, sections were incubated in biotinylated goat anti-mouse or anti-rabbit antibody (diluted 1:200, Vector Laboratories) for 1 h at room temperature. After incubation with the biotinylated secondary antibody, the avidin–biotin complex (ABC; VECTASTAIN® ABC reagent prepared in advance as described in the kit instructions) and diaminobenzidine (DAB; DAB Peroxidase Substrate Kit, Vector Laboratories) were applied to the sections for visualization of the reaction product. We used uninjured caudal sections of spinal cords from patients with CSM, which served as within-case controls to negate the issue of complicating factors, such as cardiopulmonary failure, in patients with CSM. Sections from four non-patients with CSM (age matched) were used as normal controls. For negative controls, the primary antibody was omitted or incubated with isotype-matched antibodies (1:100–1:10 000, IgG). Positive controls were sections from mice or human after spinal cord injury.

Analysis of apoptosis for human cervical spondylotic myelopathy

Spinal cord sections were processed for terminal deoxynucleotidyl transferase dUTP nick end labelling (TUNEL) (ApopTag®) plus fluorescein or a peroxidase *in situ* apoptosis detection Kit (Chemicon Biotechnology Inc), as described previously (Cregan *et al*., 2002).

Double immunostaining for human cervical spondylotic myelopathy

Double labelling with TUNEL, Fas, Fas ligand and cell specific markers was carried out to determine which cell types were undergoing apoptosis or expressing Fas and Fas ligand. Labelling was performed according to the Vector Laboratories protocol for multiple antigen labelling using ABC systems. Briefly, following TUNEL, Fas or Fas ligand staining, sections were incubated with either 2% H_2O_2, avidin solution or the biotin solution (Vector), for 15 min and rinsed with phosphate-buffered saline. Sections were then incubated in 5% milk and 1% bovine serum albumin for 1 h, and incubated with one of the following cell-specific markers overnight at 4°C: neuron-specific anti-NF200 and anti-MAP2 (1:100; Sigma); oligodendrocyte-specific anti-2′, 3′-cyclic nucleotide 3′-phosphodiesterase (CNPase; 1:200; Chemicon) or anti-APC (1:20; Calbiochem) or astrocyte specific anti-glial fibrillary acidic protein (GFAP; 1:100 dilution; Dako), myelin-specific anti-MBP (myelin basic protein; 1:1000, Boehringer Mannheim GmbH) and microglia and macrophage selective CD68; (1:50, Dako) in 15% normal goat serum for 1 h at room temperature. Sections were then incubated for 1 h in either a goat anti-mouse secondary antibody conjugated to biotin or an anti-rabbit secondary antibody conjugated to biotin (1:300, Vector) or fluorescence (1:200; Texas Red or FITC, Jackson Laboratories) conjugated anti-mouse or anti-rabbit secondary antibodies in 10% normal goat serum for 1 h at room temperature. The sections were then washed in phosphate-buffered saline and incubated with the avidin–biotin complex (ABC) complex (VECTASTAIN® ABC reagent prepared in advance as described in the kit instructions) for 30 min (Vector) in 2% normal horse serum. Tissues were then incubated for 7 min with the diaminobenzidine and a nickel solution (DAB Peroxidase Substrate Kit, Vector Laboratories) for visualization of antibody binding and to void autofluorescence in human materials. Images were captured using Nikon Eclipse E800 light and Zeiss LSM 510 META confocal microscopes (Thornwood).

Twy/twy mouse model of cervical spondylotic myelopathy

Twy/twy mice were obtained from a breeding colony of the Central Institute for Experimental Animals, Kanagawa, Japan. Mutant *twy/twy* mice were maintained by brother–sister mating of heterozygous Institute of Cancer Research mice (+/twy) (Uchida *et al*., 1998; Yu *et al*., 2009*a*). These mice, which harbour an autosomal recessive mutation in the *NPPS* gene, develop progressive spinal cord dysfunction secondary to extradural calcified deposits at C2–C3 with cervical cord compression.

Administration of anti-Fas ligand antibody in twy/twy mice

Homozygous twy/twy mice were identified by a characteristic tip-toe walking pattern that typically commences at 3 weeks of age and profound motor paresis that progresses between 4 and 7 months. Four-month-old twy/twy mice received the anti-Fas ligand antibody (CD178: anti-Fas ligand) (MFL3; BD Bioscience) as functional grade purified antibody, which is host/isotype from Armenian hamster IgG, 50 μg intra-peritoneally twice weekly for 4 weeks; plain control mice (saline), received artificial CSF twice weekly for 4 weeks as the vehicle control and IgG control mice (IgG) received 50 μg hamster

IgG1-isotype monoclonal antibody intra-peritoneally twice weekly for 4 weeks. All treatments were performed in a double-blind manner.

Footprint analysis

Functional neurological recovery was assessed by quantitative footprint analysis at weekly intervals for the 4-week treatment. Footprint analysis was modified from the method described by de Medinaceli *et al*. (1982). Briefly, the animals' forepaws and hindpaws were immersed in non-toxic red (forepaw) and green dyes (hindpaw). The mice ($n = 12$/group) were then permitted to walk across a narrow wooden board, with dimensions ~1 m long and 7 cm wide, from a brightly illuminated starting box leading to a darkened box containing their familiar housing mates. Before collecting the footprints, each mouse was allowed to freely explore the runway for 5 min. Footprint recording took place when the mouse was able to run along the runway at a steady pace and in a straight line. To collect the footprints, a fresh sheet of white paper was placed on the floor of the runway for each mouse. Toe spread was measured as the distance between the first and fifth toe in the forepaw and hindpaw as expression in centimetre, while interlimb coordination was measured as the distance between the ipsilateral forepaw (centre of pad) and hindpaw (centre of pad) and is expressed in centimetre. Stride length (the mean distance between each footprint) was determined by drawing a line between each ipsilateral forepaw footprint and measuring its length; stride width (the mean distance between left and right footprints) was determined by measuring the perpendicular distance of a given footprint to the line connecting its opposite preceding and proceeding footprints (Carter *et al*., 1999; Pallier *et al*., 2009). For each paw of each mouse, a set of four consecutive footprints was used (those from the initiation and finishing of the run were ignored). The mean value of stride length, stride width, toe spread and inter-limb coordination was averaged to a single value per mouse (from 3 to 5 samples) and then divided by the values from the first week of treatment and expressed as the percentage of change. The mean of the percentage of change for each mouse ($n = 12$/group) was used for statistical comparison. Values are expressed as the mean ± SD.

Body weight measurements

As a measure of general health, body weights were assessed at the beginning and end of the 4-week treatment period.

Immunohistochemical analysis for twy/twy mice

Twy/twy mice were perfused transcardially with 4% paraformaldehyde solution under deep anaesthesia with sodium pentobarbital (50 mg/kg Somnotol; MTC Pharmaceuticals). Cervical spinal cord segments containing the compressed region were dissected, post-fixed using 10 and 20% sucrose solutions and then embedded within Tissue-Tek® Optimal Cutting Temperature compound (Sakura Finetek). Serial transverse sections of 14 μm thickness were cut and mounted onto gelatin-subbed slides and stored at –80°C. The site of injury was defined by Luxol fast blue and haematoxylin and eosin staining of the tissue sections at 500 μm intervals. Sections were blocked in a blocking solution (0.3% Triton X-100, 5% milk and 1% bovine serum albumin in phosphate-buffered saline) for 1 h and incubated with astrocyte-selective rabbit anti-GFAP (1:100; Sigma-Aldrich), macrophage/microglia-selective rat anti-F4/80 (Santa Cruz Biotechnology) and rabbit anti-ionized calcium binding adaptor molecule 1 (Iba1, Wako Chemicals USA) antibodies in blocking solution overnight at 4°C. The slides were washed in phosphate-buffered saline three times and incubated with fluorescent Alexa 594 or 488 anti-mouse, anti-rabbit or anti-rat secondary antibodies (1:200; Sigma-Aldrich) for 1 h. Staining specificity was determined both by omitting the primary antibody and by competing the primary antibody with its corresponding peptide prior to incubation.

Western blotting in twy/twy mice

Spinal cord samples of 1 cm length centred at the injury site were extracted from twy/twy mice ($n = 5$ per group) for total proteins. Spinal cords were individually homogenized in a buffer (5 mM Tris–HCl, 4 mM EDTA, 1 μM pepstatin, 100 μM leupeptin, 100 μM phenylmethylsulphonylfluoride and 10 μg/ml aprotinin) at 4°C. All protein samples were resolved (20–50 μg per lane) in a 12% sodium dodecyl sulphate–polyacrylamide gel at 200 V. Proteins were transferred to a nitrocellulose membrane. Membranes were blocked with 5% non-fat milk in Tris–buffered saline–Tween-20 for 1 h and incubated with: (i) rabbit anti-NF200 (1:1000, Sigma); (ii) mouse anti-microtubule associated protein-2 (MAP2, 1:200, Sigma); (iii) mouse anti-β-III tubulin (1:400, Chemicon); (iv) rabbit anti-caspase-9 (Cell Signalling Technology); (v) Bcl-2 (1:200, Cell Signalling); (vi) rabbit anti-GFAP (1:1000, Chemicon) and (vii) rabbit anti-Iba1 antibody (1:400, Wako Chemicals USA). Membranes were washed and then incubated for 1 h in the presence of anti-mouse (1:4000) or anti-rabbit (1:2000) secondary antibody conjugated to horseradish peroxidase. Reaction products were visualized using an ECL western blot detection kit (Amersham Biosciences Inc) and exposed to film. To quantify the amount of protein, the bands were determined to be within the linear range of the radiographic film, and optical densities were then determined by measuring the integrated optical density across the band using Gel Pro analysis software (Media Cybernetice). Densitometric values were normalized to those of β-actin (1:400; Sigma). Western blot analysis confirmed Iba1, GFAP, Caspase-9, NF200 and anti-β-III tubulin expression derived from Institute of Cancer Research, saline, anti-Fas ligand ($n = 5$/group) and IgG ($n = 6$ groups) mice. The mean value of each sample from 3 to 5 repeat experiments was averaged to a single value per mouse for Iba1, GFAP, Caspase-9, NF200 and β-III tubulin expression to statistical comparison and expressed as the mean ± SD ratio.

Cell quantification for human cervical spondylotic myelopathy

All digital images were acquired in a double-blind manner. Digital images were captured from two random fields per section from the epicentre of compression and uncompressed caudal region of cases with CSM, and control cases using a Nikon Eclipse E800 light microscope ×20 objective for CD68 and Iba1-positive cells and ×10 objective for Fas, Fas ligand and MAP2-positive neurons. We counted digital images of CD68, Iba1, Fas, Fas ligand and MAP2-positive cells in two fields per section using ImageJ software (developed at the National Institute of Health). Values from two fields were averaged to a single value per case for CD68, Iba1, Fas, Fas ligand and MAP2. The results were expressed as the number of CD68 and Iba1-positive cells and the number of Fas, Fas ligand and MAP2-positive neurons per ×20 or ×10 field. To assess the number of TUNEL-positive cells, digital images were captured in five random fields per section from the epicentre of compression and uncompressed caudal regions of cases with CSM, and control cases in spinal cord grey and white matter at ×20 objective using a Nikon Eclipse E800 light microscope. We then counted the number of TUNEL-positive cells and expressed as total values per case in grey matter and white matter, respectively.

Statistical analysis

Significant differences in cell counts were analysed with repeated measures ANOVA and *t*-test using the Statistical Package for the Social Sciences (SPSS SigmaStat 3.0) (Aspire Software International). All data are expressed as mean ± SD. The criterion for significance was set at $P < 0.05$.

Results

Clinical data

The clinical and pathologic data are summarized in Table 1. The ages of the patients ranged from 61 to 89 years (mean age 73 years), and time from CSM onset to death ranged from 6 months to 50 years.

Histopathological findings in human cervical spondylotic myelopathy

We analysed cross-sections of the cervical cord obtained from eight autopsied patients whose post-mortem interval ranged between 1 and 30 h. Luxol fast blue staining revealed uniformly myelinated tracts of white matter in control cases (Fig. 1). However, flattening and indentation of the spinal cord and severe anterior and posterior horn atrophy, neuronal loss, axonal loss and swellings, myelin pallor, gliosis and vacuolations were observed in the compressed epicentre from the six most severely damaged spinal cords of patients with CSM. Demyelination was observed in the descending axons of the lateral pyramidal tract and degeneration of ascending fibre tracts was observed in the posterior columns. Dorsal root degeneration and gliosis were also observed. In a case examined at 6 months after the onset of CSM, haematoxylin and eosin and Luxol fast blue stained spinal cord tissue revealed atrophy and loss of neurons in anterior horn, loss of axons and myelin and vacuolation in both sides of the lateral corticospinal tracts (Fig. 1D, inset box). In addition, dense and disordered myelin was distributed in intact white matter. Four to five years after the onset of CSM, abnormal thickening of the vessels in grey matter and severe myelin pallor in the white matter of the spinal cord were observed when compared with control cases. Eight to 10 years after the onset of CSM, the spinal cord had a flattened appearance, with demyelination and vacuolation in the posterior column (Fig. 1H, inset box) and intense myelin staining in non-degenerated areas. In a case examined 50 years after the onset of CSM, atrophy of the anterior horn and marked loss of neurons and myelin in the compressed epicentre were observed when compared with control cases.

Axonal damage and anterior horn atrophy in human cervical spondylotic myelopathy

We observed severe anterior horn atrophy with neuronal loss (Fig. 1, *left*: 6 months, 4 years and 10 years), and axonal swellings and loss in white matter of CSM spinal cords at 6 months (Fig. 1D) and 10 years (Fig. 1H). The number of MAP2-positive motor neurons was significantly lower within the severely compressed epicentre of the spinal cords when compared with non-compressed caudal regions of the spinal cord in the cases with CSM ($P = 0.001$) or from sections of spinal cord taken from control cases ($P = 0.005$) (Fig. 1I). The compressed spinal cord was also characterized by a decreased density of NF200-positive axons (Fig. 1D and H). Moreover, there was an increase in the number of β-APP-positive degenerating axons in the white matter at the compressed epicentre of the spinal cords from patients with CSM when compared with control spinal cords (Fig. 1J and K).

Fas expression in the compressed epicentre of human cervical spondylotic myelopathy

To determine whether chronic spinal cord compression induces Fas expression, we performed immunohistochemistry with an anti-Fas antibody. A small number of Fas-positive cells were observed in control spinal cords (Fig. 2A) and in the caudal spinal cord of cases with CSM (Fig. 2B). In contrast, we observed many Fas-positive cells in the grey and white matter at the epicentre of all CSM spinal cords. Double-labelling with Fas and cell-specific markers revealed Fas immunoreactivity in neurons (Fig. 2C), astrocytes (Fig. 2D), microglia/macrophages (Fig. 2E) and oligodendrocytes (Fig. 2F) in the compressed epicentre of spinal cords from cases with CSM. Between 6 months and 4 years after the onset of CSM, Fas-positive cells mainly consisted of macrophages and astrocytes at the epicentre of compression in CSM spinal cords. Between 10 and 50 years after the onset of CSM, Fas-positive motoneurons could still be observed in the epicentre of CSM spinal cords but not in the uninjured caudal regions of CSM spinal cords. Furthermore, the number of Fas-positive neurons (10.2 ± 5.76) was significantly higher in the injury epicentre when compared with control spinal cords and the caudal spinal cord of cases with CSM (1.5 ± 0.75, $P = 0.002$) (Fig. 2L).

Expression of Fas ligand in the compressed epicentre of human cervical spondylotic myelopathy

To determine whether chronic spinal cord compression induces Fas ligand expression, we employed immunohistochemistry with an anti-Fas ligand antibody. We found little Fas ligand immunoreactivity in control spinal cords (Fig. 2G). However, in the non-compressed caudal regions of spinal cords from cases with CSM, there was a slight increase in the number of Fas ligand-positive cells (Fig. 2H). By 6 months after CSM, we observed many Fas ligand-positive cells in the compressed cervical spinal cord of cases with CSM. By double labelling with Fas ligand and cell-specific markers, we determined that Fas ligand immunoreactivity was mainly expressed in neurons (Fig. 2I) and astrocytes (Fig. 2J) in the epicentre of CSM spinal cords. Between 4 and 50 years after the onset of CSM, despite markedly reduced

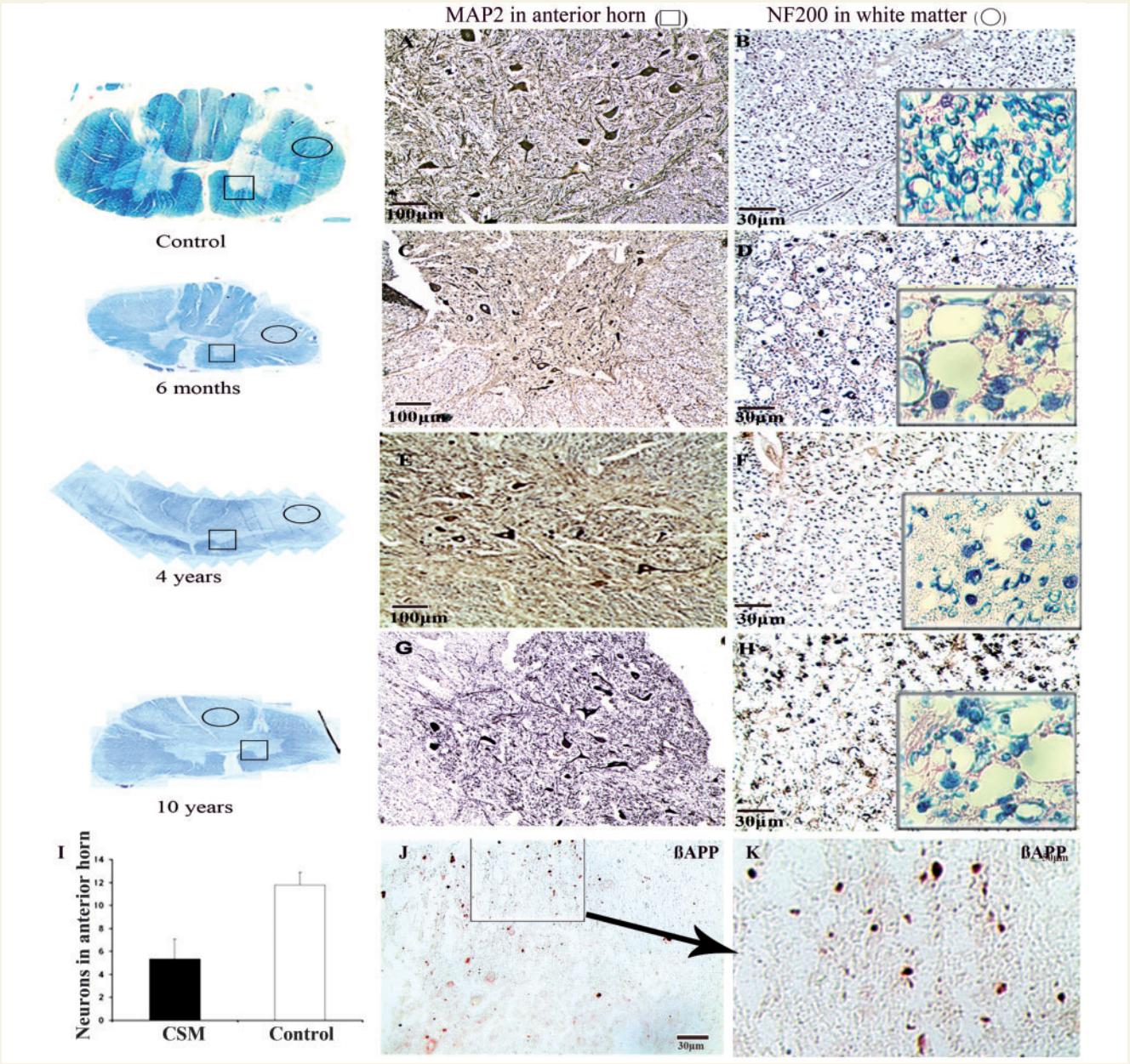

Figure 1 Axonal degeneration and neuronal loss in the compressed epicentre of CSM lesions. Using haematoxylin and eosin and Luxol fast blue staining and immunochemistry with NF200 and MAP, we observed severe anterior horn atrophy, neuronal loss (*left*: 6 months, 4 years and 10 years and **C**, **E** and **G**), axonal swellings and vacuolation in the white matter at 6 months (**D**) and 10 years (**H**) when compared with normal controls (**A** and **B**). At 4 years, decreased axonal density (**F**) was observed in the white matter in the epicentre of CSM spinal cords when compared with control cases (**B**). The number of MAP2-positive motoneurons (**I**) was significantly decreased in the epicentre when compared with control case. Furthermore, β-APP positive damaged axons were seen in the epicentre of CSM spinal cords (**J** and **K**).

expression of Fas ligand-positive astrocytes when compared with 6 months, we noted a moderate increase in the number of activated microglia/microphages in degenerated white matter (Fig. 2K). Furthermore, the number of Fas ligand-positive neurons was significantly higher in the compressed epicentre (5.85 ± 3.38) in all eight cases of CSM when compared with control spinal cords or the caudal spinal cord from cases with CSM ($P = 0.001$) (Fig. 2M).

Neural apoptosis is prominent in the compressed cervical cord in human cervical spondylotic myelopathy

To determine whether the chronic non-traumatic spinal cord injury caused by CSM induces apoptosis, we employed TUNEL labelling. We observed no TUNEL-positive cells in control spinal cords (Fig. 3A)

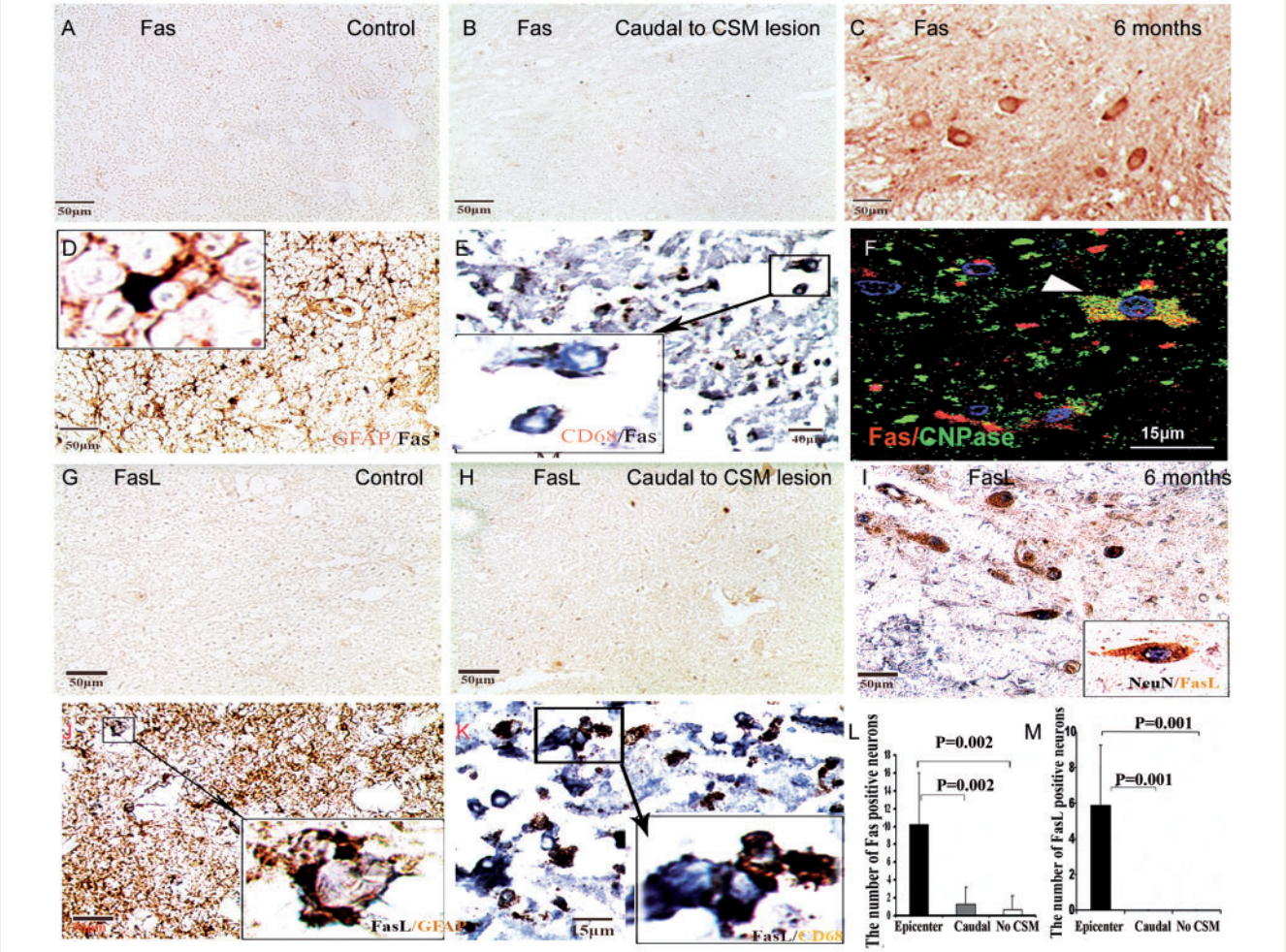

Figure 2 Fas and Fas ligand expression in the spinal cords of humans with CSM. In control cases and in caudal to CSM lesion from patients with CSM, Fas and Fas ligand-positive cells were scarce (**A**, **B**, **G** and **H**). Using double labelling with cell-specific markers, there are many Fas-positive neurons (**C**), astrocytes (**D**), macrophages (**E**) and oligodendrocytes (**F**) around the epicentre of compression in the spinal cords of patients with CSM at 6 months after CSM onset. We also found Fas ligand-positive neurons (**I**), astrocytes (**J**) and microglia/macrophages (**K**) in the spinal cords of patients with CSM. The number of Fas (**L**) ($P = 0.002$) and Fas ligand (**M**) ($P = 0.001$) positive neurons was significantly higher in the injury epicentre of CSM ($n = 8$) when compared with control spinal cords ($n = 4$) and uncompressed regions to CSM lesion.

and only a small number of TUNEL-positive cells in the caudal spinal cord of cases with CSM (Fig. 3B). We observed that most apoptotic cells were randomly distributed in the epicentre of compression in CSM spinal cords at 6 months (Fig. 3C), 4 and 10 years after CSM diagnosis. Remarkably, 50 years after the onset of CSM, TUNEL-positive cells could still be seen in the cervical cord of cases with CSM. Quantitative analysis showed a significant increase in the number of TUNEL-positive cells in white matter and grey matter in the lesion epicentre of cases with CSM when compared with caudal regions of the cord from cases with CSM or the cervical cord from control cases ($P < 0.05$, Fig. 3D). We performed double labelling with cleaved caspase-3, TUNEL and cell specific markers to determine which cell types were undergoing apoptosis. We confirmed the presence of myelin basic protein-positive oligodendrocytes that co-expressed cleaved caspase-3 (Fig. 3E), TUNEL-positive neurons (Fig. 3F) and microglia/macrophages (Fig. 3G) in the lesion epicentre of cases with CSM. Quantification with cell specific labelling revealed that 12% of the TUNEL-positive cells were neurons, 19% were oligodendrocytes and 29% were macrophages. Clear double labelling could not be identified in the remaining 40% of cells, potentially due to progressive degradation of cellular integrity due to pre-mortem biological effects or due to length of storage in paraffin blocks/pathology archive. Furthermore, we also found activated caspase-3 positive cells at 6 months (Fig. 3H) and 50 years (Fig. 3I) and activated caspase-9 (Fig. 3J) and -7 (Fig. 3K) positive cells in the epicentre of CSM spinal cords.

Fas/Fas ligand-mediated apoptosis in human cervical spondylotic myelopathy

To confirm that Fas expression is associated with apoptotic cell death, we performed double-labelling experiments with TUNEL and anti-Fas antibody. We observed that Fas-positive cells

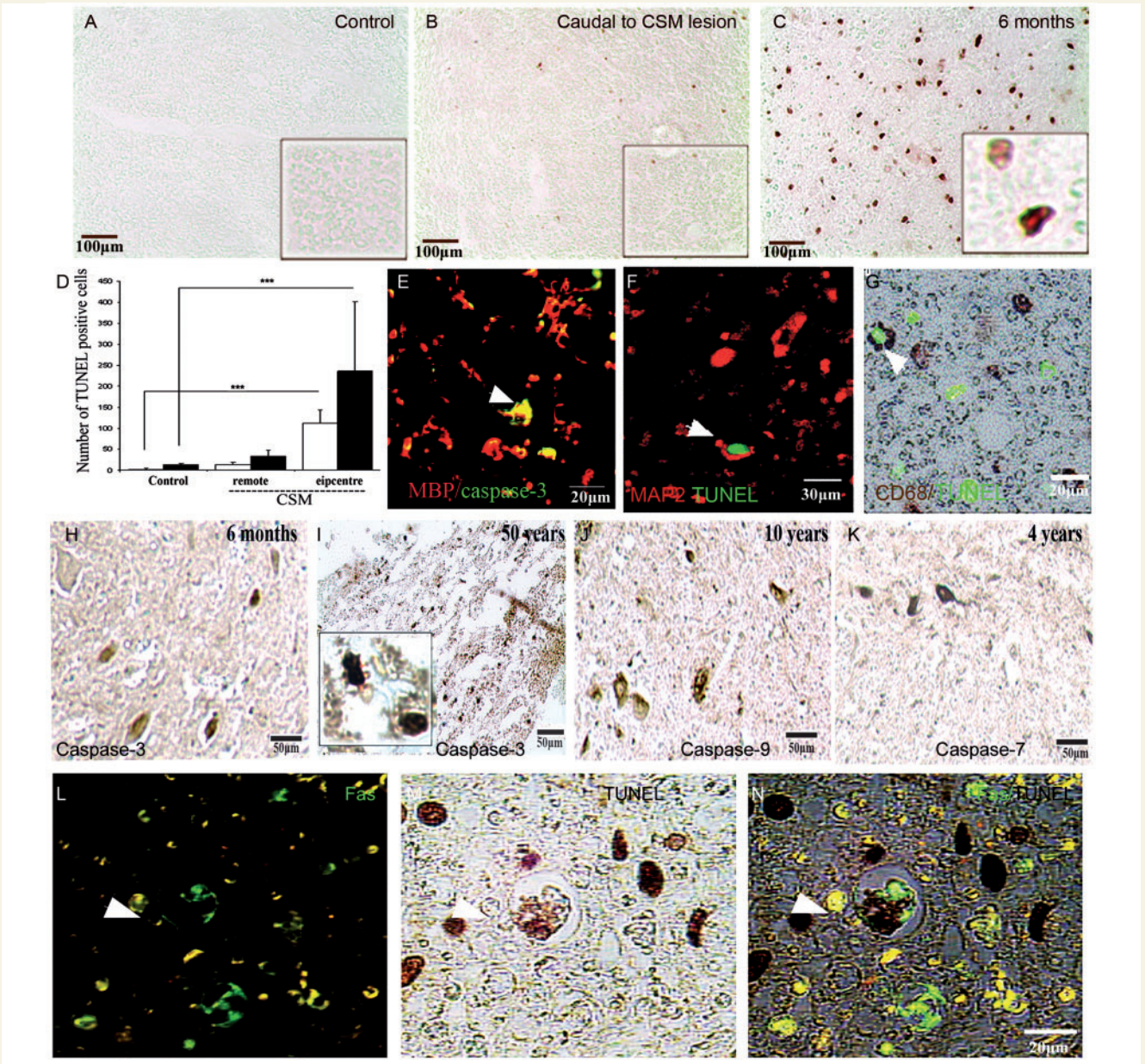

Figure 3 Apoptosis and Fas mediated apoptosis in the spinal cords of humans with CSM. No TUNEL-positive cells were observed in control cases and a few could be seen in caudal to CSM lesion (**A** and **B**). We observed that most apoptotic cells were distributed in the epicentre of CSM spinal cords (**C**) at 6 months. The quantification of apoptotic cells showed a significant increase in the number of TUNEL-positive cells in CSM when compared with caudal to CSM lesion ($n = 8$) and ($n = 4$) control cases ($P < 0.05$, **D**) (white bar = white matter; black bar = grey matter). Double labelling with cell-specific markers and cleaved caspase-3 or TUNEL was used to demonstrate TUNEL-positive oligodendrocytes (**E**), neurons (**F**) and microglia/macrophages (**G**) in the epicentre of compression of CSM. We observed activated caspase-3 positive cells (**H** and **I**) and activated caspase-9 (**J**) and -7 (**K**) positive cells in the epicentre of CSM spinal cords. To confirm that Fas expression is associated with apoptotic cell death, we performed double-labelling experiments with TUNEL (**M**) and anti-Fas antibody (**L**). We observed that Fas-positive cells co-labelled with TUNEL in the white matter of spinal cords from patients with CSM (**N**).

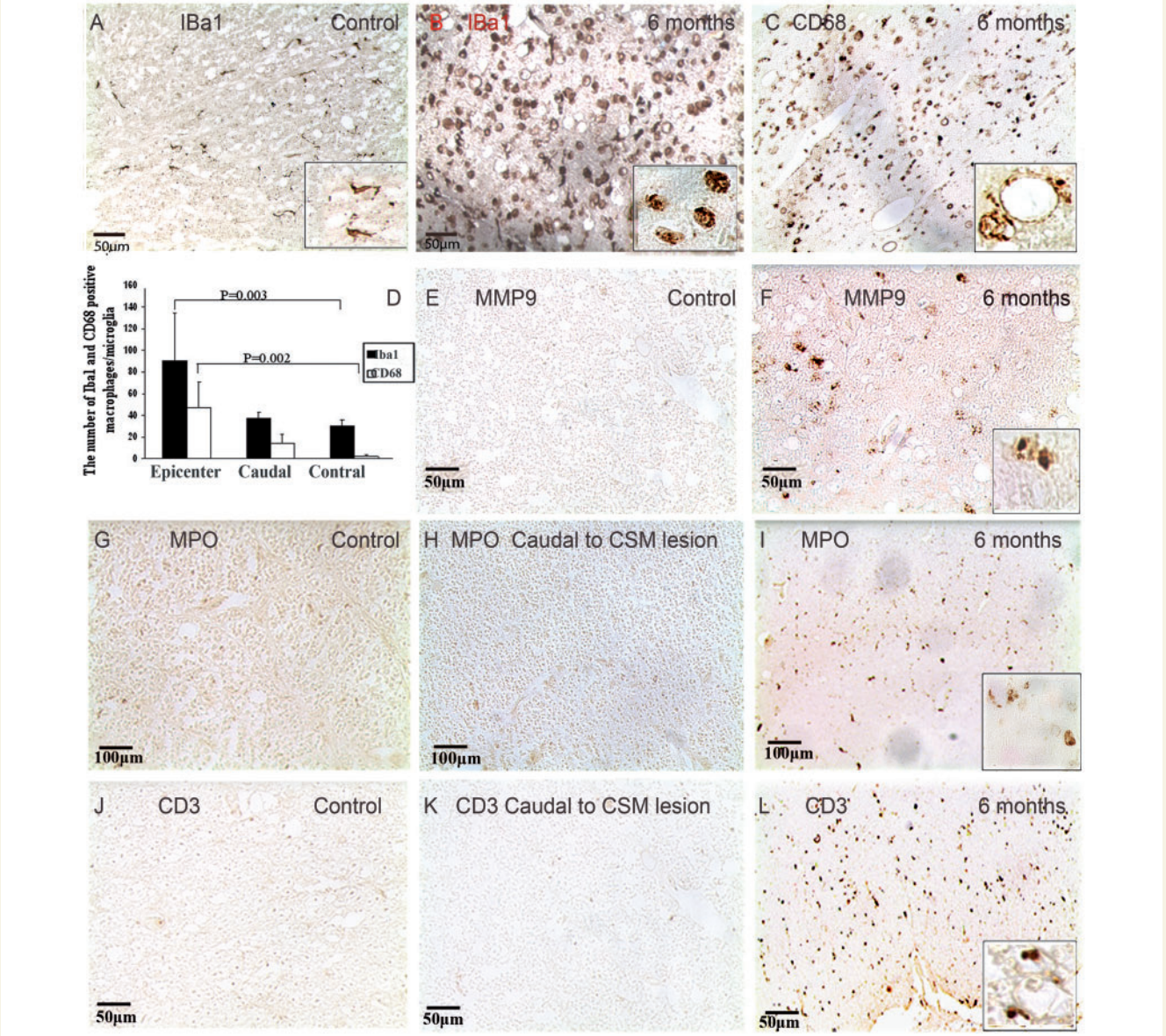

Figure 4 Inflammation in the spinal cord of humans with CSM. In control cases, Iba1-positive microglia were scarce (**A**). There are many Iba1 (**B**) and CD68 (**C**) positive macrophages in the epicentre of compression at 6 months after CSM. The number of Iba1 and CD68 positive microglia/macrophages was significantly greater in the epicentre of CSM spinal cords when compared with controls ($P = 0.003$ and $P = 0.002$, respectively, **D**) ($n = 8$ cases of CSM and $n = 4$ control cases). No MMP9 positive cells were observed in control cases and caudal to CSM lesion (**E**). However, MMP9-positive cells were also observed in the epicentre of compression (**F**). There are few CD3 and myeloperoxidase (MPO) positive cells in control case (**G** and **J**) and caudal (**H** and **K**) to CSM lesion. However, many myeloperoxidase (**I**) positive cells and CD3 (**L**) positive lymphocytes were found throughout the lesioned spinal cord parenchyma in a human subject with a 6 month history of CSM.

co-labelled with TUNEL (Fig. 3N) in the white matter of spinal cords from patients with CSM.

Time course and Fas-mediated inflammatory response in human cervical spondylotic myelopathy

To determine the role of Fas ligand in the modulation of immune reactions involving macrophages, immunohistochemistry was undertaken with antibodies to Iba1 (resident microglia/macrophages), CD68 (activated macrophages), CD3 (T-lymphocytes), myeloperoxidase (neutrophils) and MMP9 (matrix metalloproteinases). We demonstrated that Iba1 and CD68 immunoreactivity was evenly distributed throughout the processes of ramified microglia with thin processes in both the grey matter and white matter in control spinal cords (Fig. 4A) and caudal regions of CSM spinal cords. However, many Iba1 (Fig. 4B) and CD68-positive cells (Fig. 4C) with larger, rounded and shorter processes, typical of activated microglia/macrophages, could be seen in the

degenerated white matter of spinal cords 6 months after the onset of CSM. Four years after CSM, many Iba1 and CD68 positive ramified microglia could be seen. At 10 and 50 years, despite the reduced expression of CD68 positive, lipid-laden, 'foamy' macrophages, a moderate increase in the number of activated microglia/microphages was observed in areas of axonal degeneration in the white matter. The number of CD68 positive microglia/macrophages was significantly higher in the compressed epicentre (47.14 ± 23.41) of CSM spinal cords when compared with caudal regions (14 ± 8.51) of CSM and normal spinal cords (2.25 ± 1.71) ($P = 0.003$, Fig. 4D). We found that the number of Iba1-positive microglia/macrophages was significantly higher at the epicentre of CSM spinal cords when compared with the number of CD68 positive microglia/macrophages ($P = 0.002$, Fig. 4D). Furthermore, we also observed several MMP9-positive neurons and microphages in the epicentres of CSM spinal cords at 6 months (Fig. 4F) but not in control cases (Fig. 4E). To confirm our findings with regards to Fas-mediated inflammation, we carried out double-labelling with CD68, Fas and Fas ligand antibodies. We identified the colocalization of Fas with CD68 (Fig. 2E) and Fas ligand with CD68 (Fig. 2K) in the compressed epicentre of CSM spinal cords. We found no myeloperoxidase-positive cells in control cases or in caudal regions of CSM spinal cords (Fig. 4G and H). However, at 6 months after CSM, we observed numerous myeloperoxidase-positive cells distributed throughout the spinal cord parenchyma, including phagocytic foamy macrophages and many intensely stained ramified and activated microglia/macrophages (Fig. 4I). Four years after CSM, many myeloperoxidase positive-activated microglia were distributed in the spinal cord parenchyma. At 50 years of CSM, only scattered solitary myeloperoxidase-positive cells were seen in the spinal cord parenchyma. Furthermore, there were few CD3-positive cells in control cases and caudal regions (Fig. 4J and K) of CSM spinal cords. Six months after CSM, however, many CD3-positive lymphocytes were seen; mostly throughout the spinal cord parenchyma (Fig. 4L). Four and 10 years after CSM, small groups of CD3-positive cells were observed to be randomly distributed in the spinal cord parenchyma, near blood vessels, and in the perivascular space at the margin of the cystic cavity. Fifty years after CSM, we detected scattered solitary CD3-positive cells in the spinal cord parenchyma.

Macrophage/microglial infiltration in twy/twy mice

We observed numerous Iba1-positive microglia/macrophages distributed in the twy/twy compressed epicentre (Fig. 5B saline and 5C IgG) in comparison with normal control mice (Fig. 5A normal). Neutralization of Fas ligand by a function blocking-antibody in twy/twy mice reduced the number of Iba1-positive macrophages and reactive microglia at the lesion sites relative to saline controls by immunohistochemistry (Fig. 5D). Western blot analysis demonstrated a reduction in levels of Iba1-protein expression in twy/twy mice treated with a function-blocking antibody relative to saline control and IgG controls in twy/twy mice (Fig. 5I and J).

Glial fibrillary acidic protein-positive gliosis in twy/twy mice

We have previously reported a significant increase in the number of the GFAP-positive astrocytes, which were conspicuously present within the grey matter of the twy/twy lesioned area (Yu *et al*., 2009*a*) in comparison to normal control mice (Fig. 5E, normal). In the present study, we found an increased number of GFAP-positive astrocytes (Fig. 5F saline and 5G IgG) of twy/twy mice. However, neutralization of Fas ligand by a function-blocking antibody in twy/twy mice reduced the number of the GFAP-positive astrocytes (Fig. 5H anti-Fas ligand) and levels of GFAP protein expression when compared with saline control of twy/twy mice by immunohistochemistry and western blot analysis (Fig. 5I and K).

Apoptosis in twy/twy mice

This is consistent with previous results obtained from our laboratory showing a significant increase in activation of caspase-9 expression in twy/twy mice compared with normal control mice (Yu *et al*., 2009*a*). Of note, neutralization of Fas ligand in the twy/twy mouse model of CSM resulted in a reduction in caspase-9 activation (Fig. 5L and M) and increase in Bcl-2 expression (Fig. 5L and N) compared with IgG controls by western blot analysis.

Changes of neurons and axons in twy/twy mice

Levels of NF200, consistent with previous results obtained from our laboratory, showing expression in twy/twy mice were significantly decreased relative to normal control mice (Yu *et al*., 2009*a*). Neutralization of the Fas ligand with a function-blocking antibody in twy/twy mice reduced loss of neurons and axons as determined by western blot analysis with NF200 (Fig. 5O and P) and β-III tubulin (Fig. 5O and Q) antibodies compared with saline control of twy/twy mice.

Neurological dysfunction in twy/twy mice

Consistent with previous results obtained from our laboratory, footprint analysis of Institute of Cancer Research mice revealed highly coordinated forelimb and hindlimb foot placements (Fig. 6A and F). In contrast, twy/twy mice showed increased ipsilateral forelimb–hindlimb distance (interlimb coordination) when compared with normal control mice (Yu *et al*., 2009*a*). Neutralization of Fas ligand by a function-blocking antibody in the twy/twy mouse model of CSM reduced changes in inter-limb coordination at 4 weeks when compared with saline ($P < 0.001$) and IgG controls ($P < 0.001$) (Fig. 6F). Anti-Fas ligand treatment in twy/twy mice reduced per cent stride length changes when compared with IgG mice (forepaws, $P < 0.003$ at 2 weeks; $P < 0.009$ at 4 weeks) and saline (forepaw, $P < 0.001$ at 2 weeks; $P < 0.011$ at 4 weeks; Fig. 6G). Anti-Fas ligand treatment in twy/twy mice also prevents the progression of locomotor dysfunction relative to saline of twy/twy mice as measured by per cent change of toe spread at 3 weeks (forepaw: $P < 0.003$;

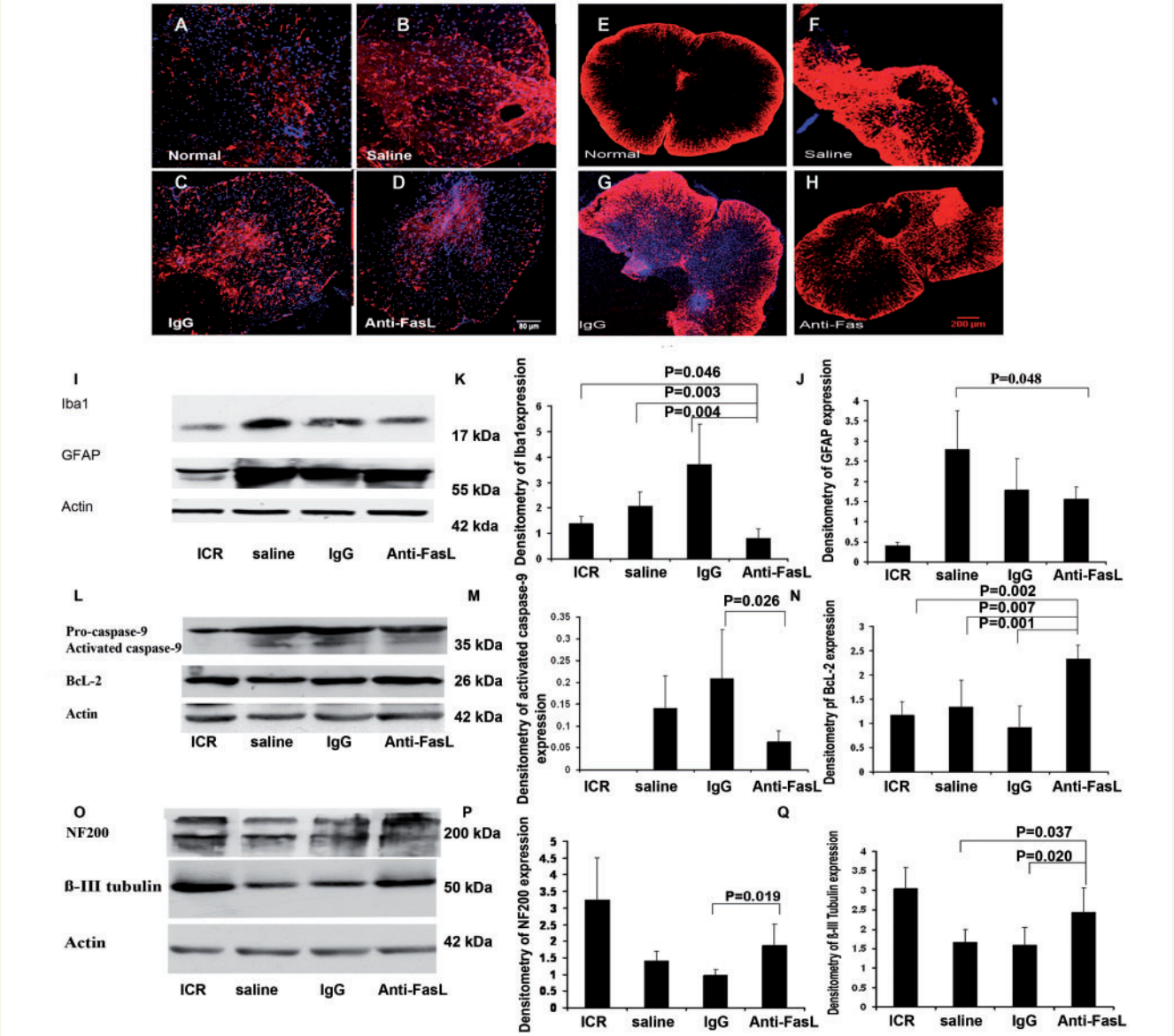

Figure 5 Neutralization of Fas ligand in the twy/twy mice reduces inflammation, apoptosis and neurodegeneration. There is an increased number of Iba1 positive microglia/macrophages in saline (**B**) and IgG (**C**) of twy/twy mice when compared to Institute of Cancer Research (ICR) control mice (**A**). We also found increased the number of GFAP-positive astrocytes in saline (**F**) and IgG (**G**) of twy/twy mice when compared to ICR control mice (**E**). However, anti-Fas ligand treatment in twy/twy mice reduced the number of Iba1-positive microglia/macrophages (**D**) and GFAP-positive astrocytes (**H**) when compared with saline and IgG of twy/twy mice, as demonstrated by immunohistochemistry. Using western blotting with Iba1, GFAP, caspase-9, BcL-2, NF200 and β-III Tubulin antibodies, anti-Fas ligand (FasL) treatment in twy/twy mice reduces densitometry of Iba1 (**I** and **J**), GFAP (**I** and **K**), caspase-9 activation (**L** and **M**) expression and increases BcL-2 expression (**L** and **N**), promotes the preservation of neurons and axons (**O**, **P** and **Q**) as compared with saline and IgG in twy/twy mice. Densitometric values were normalized to those of β-actin (1:400; Sigma). Western blot analysis confirmed Iba1, GFAP, caspase-9, NF200 and Tubulin expression derived from ICR saline, anti-Fas ligand ($n = 5$/group) and IgG ($n = 6$ groups) mice. The mean of each sample from several (3–5) experiments was used for statistical comparison and expressed as the mean ± SD ratio.

Fig. 6H). Furthermore, anti-Fas ligand treatment in twy/twy mice limited changes in per cent stride width in the forepaws when compared with saline-treated animals ($P < 0.016$ at 3 weeks; $P < 0.003$ at 4 weeks) and IgG treatment ($P < 0.025$ at 4 weeks) (Fig. 6I). While the toe spread and stride width of the hindpaws in anti-Fas ligand treatment mice did not differ from that of their saline and IgG littermates. All data are from Institute of Cancer Research, saline, IgG and anti-Fas ligand treatment in twy/twy mice ($n = 12$ mice/groups). Moreover, neutralization of Fas ligand by a function-blocking antibody in the twy/twy mouse model of CSM attenuated weight loss (Fig. 6J) and improved functional neurological recovery relative to IgG control ($P < 0.042$) of twy/twy mice. The data suggest that intervention to inhibit the Fas pathway may substantially improve outcome and prevent the progression of locomotor dysfunction.

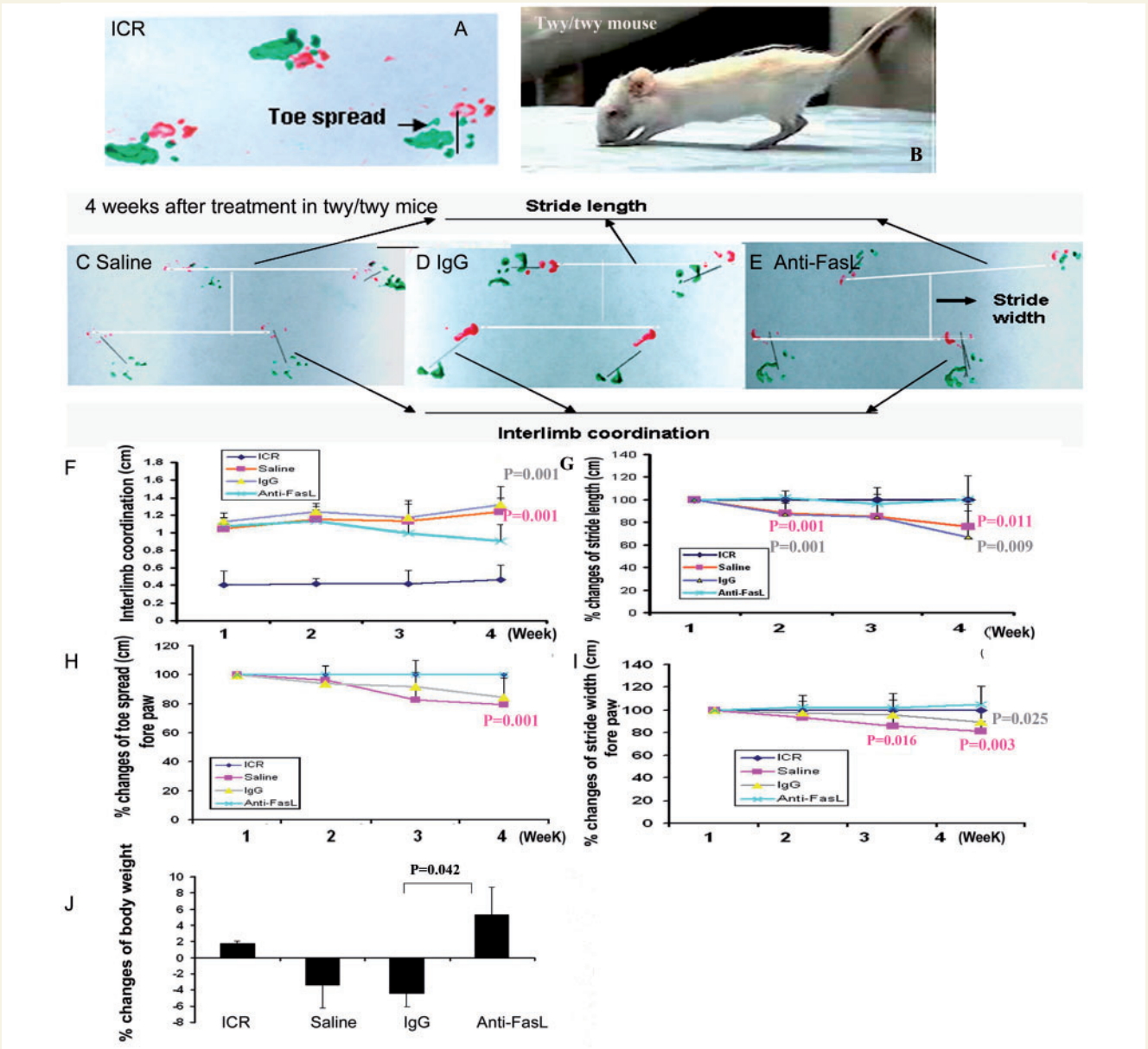

Figure 6 Anti-Fas ligand treatment in the twy/twy mice improved functional neurological recovery. A comparison of the walking track footprints was made for Institute of Cancer Research (ICR) control mice (**A**) and saline (**C**), IgG (**D**) and anti-Fas ligand (**E**) after 4 weeks treatment in twy/twy mice. (**B**) Four-month-old twy/twy mouse. Quantification of distance between ipsilateral forepaw (centre of pad) and hindpaw (centre of pad) as inter-limb coordination, the first and fifth toe in the forepaw and hindpaw as toe spread, stride length and stride width were calculated and plotted. Data are from Institute of Cancer Research, saline, IgG and anti-Fas ligand treatment in twy/twy mice ($n = 12$ mice/groups). Anti-Fas ligand treatment in the twy/twy mice improved in interlimb coordination at 4 weeks (**F**), per cent change of stride length at 2 and 4 weeks (**G**), per cent change of toe spread at 3 weeks (**H**: forepaw) and percentage change of stride width at 3 and 4 weeks (**I**) when compared saline and IgG group. Furthermore, anti-Fas ligand treatment in the twy/twy mice also reduces weight loss (**J**) relative to IgG ($P = 0.042$) treated twy/twy mice. Results are expressed as the mean ± SD.

Discussion

Our data provide strong evidence implicating a role for Fas-mediated apoptosis in the pathobiology of CSM. The human neuropathology data point to the association of Fas expression with ongoing neuronal and oligodendroglial apoptosis, which is further characterized by persisting inflammation, demyelination and neuronal/axonal loss. Moreover, blocking Fas ligand with a Fas function-blocking antibody in a murine model of CSM dramatically improves neurobehavioural function, attenuates Fas-mediated neural apoptosis and reduces the neuropathological consequences of cord compression. These data strongly suggest that targeting the Fas pathway is an attractive therapeutic target to treat patients with CSM, which is complementary to existing surgical decompressive strategies.

A growing body of evidence demonstrates that apoptosis plays an important role in determining neurological outcome after spinal cord injury based on studies in humans and clinically relevant animal models (Li *et al*., 1996, 1999; Crowe *et al*., 1997; Emery *et al*., 1998; Lou *et al*., 1998; Springer *et al*., 1999; Casha *et al*., 2001; Keane *et al*., 2001). The death receptor Fas has gained widespread recognition as a critical regulator of apoptosis (Felderhoff-Mueser *et al.,* 2000; Desbarats *et al.,* 2003; Demjen *et al.,* 2004; Casha *et al.,* 2005) following spinal cord injury. We and others have shown that neuronal, oligodendrocytic and microglial apoptosis, through activation of the Fas death receptor pathway, is a key event following spinal cord injury (Casha *et al*., 2001; Zurita *et al*., 2001; Yamaura *et al*., 2002; Demjen *et al*., 2004; Yoshino *et al*., 2004) and in animal models of CSM (Yu *et al*., 2009*a*). Fas deficiency (Yoshino *et al*., 2004; Casha *et al*., 2005), the neutralization of endogenous Fas ligand (Demjen *et al*., 2004; Yu *et al*., 2009*a*) and deletion of Fas ligand in myeloid cells (Letellier *et al*., 2010) have been shown to decrease apoptosis in neurons and oligodendrocytes and to greatly decrease the number of neutrophils and macrophages infiltrating the injured spinal cord and improve functional recovery following spinal cord injury. Furthermore, there are significant histopathological and pathophysiological similarities between CSM and traumatic spinal cord injury (Fehlings and Skaf, 1998). We and others have shown that apoptosis of neurons and oligodendrocytes caused by activation of death-promoting caspases is observed at the most compressed site of twy/twy mice, an animal model of CSM, as well as in case reports of patients with CSM (Yamaura *et al*., 2002; Yu *et al*., 2009*a*). Apoptosis plays a central role in delayed demyelination and axonal dysfunction, leading to the development of neurological deterioration in CSM. In the present study, we observed a large number of apoptotic oligodendrocytes and neurons in of the spinal cords of all cases with CSM. Specifically, we observed 19% neuronal apoptosis in the epicentre of compression in CSM spinal cords with a time course from 6 months to 50 years when compared with control cases and caudal regions of CSM spinal cords. Our data provide evidence that a significant consequence of spinal cord compression is the loss of cells due to apoptosis, leading to spinal cord dysfunction, which is associated with loss of neurons and oligodendrocytes, demyelination and reactive astrogliosis. There are several factors that may contribute to oligodendrocytic and neuronal apoptosis 6 months to 50 years after the onset of CSM. First, the decreases in spinal cord blood flow and ischaemia that result from cervical spinal stenosis may be an important event that initiates apoptosis (the sensitivity of neurons and oligodendrocytes) in CSM. Second, there is a significant increase in Fas/Fas ligand-positive neurons in compressed epicentre when compared with control cases and caudal regions of CSM spinal cords. We also confirmed many activated caspase-3, 7 and 9 positive neurons in the compressed epicentre of CSM spinal cords and the co-localization of Fas and TUNEL in the degenerated white matter of CSM spinal cords, which suggests that Fas-mediated apoptosis plays an important role in neuronal degeneration in CSM. Furthermore, the neutralization of Fas ligand resulted in a reduction of caspase-9 activation, demyelination, upregulation of the anti-apoptotic factor Bcl-2, and improved functional neurological recovery in twy/twy mice. These findings represent the first evidence suggesting that the targeting of a death receptor pathway is a viable neuroprotective strategy, and demonstrate that neurons and glia (specifically, oligodendrocytes) are targets for neuroprotection in CSM. Our findings may lead to better therapeutic strategies to improve neuronal and oligodendrocyte survival, and thus may improve neurological outcome in patients suffering from CSM.

The inflammatory response following neurotrauma is a complex phenomenon involving the activation of resident microglia and the infiltration of neutrophils, monocytes/macrophages and lymphocytes into the lesion from the systemic immune system (Popovich *et al*., 1997; Hausmann, 2003). This leads to tissue damage, demyelination and neurological dysfunction (Giulian and Corpuz, 1993; Jones *et al*., 2005) as well as enhancement of Fas-mediated apoptosis of neurons and oligodendrocytes after spinal cord injury (Spanaus *et al*., 1998; Badie *et al*., 2000; Pouly *et al*., 2000; O'Connell *et al*., 2001). Fas-induced inflammatory responses in astrocytes can exacerbate Fas-mediated tissue damage by increasing the proliferation and migration of immune cells into the CNS (Choi *et al*., 2003). Apoptotic cells may release neurotoxic molecules and cytokines that stimulate microglia and the infiltration of neutrophils, monocytes/macrophages and lymphocytes into the lesion from the systemic immune system (Popovich *et al*., 1999; Mabon *et al*., 2000), leading to further tissue damage, demyelination and neurological dysfunction (Giulian and Corpuz, 1993; Jones *et al*., 2005). Fas-induced inflammatory responses in astrocytes can exacerbate Fas-mediated tissue damage by increasing proliferation and migration of immune cells into the CNS (Choi *et al*., 2003). Identifying the key triggers of apoptosis in CSM, as we have shown here, and developing approaches to block these cell-death programmes, are major challenges in the field. However, the involvement of Fas activation in the initiation of apoptosis and inflammation in the setting of CSM has been less clear prior to these results. We detected Fas and Fas ligand-positive astrocytes at the epicentre of compression in the spinal cords of patients with CSM, from 6 months to 4 years after onset. This is in agreement with previous findings that have shown that astrocytes may be resistant to Fas-mediated cell death (Becher *et al*., 1998) and instead produce proinflammatory cytokines and chemokines upon Fas ligation, which can induce Fas-mediated neuronal and oligodendrocytic apoptosis, possibly leading to neurodegeneration and demyelination. Exclusive deletion of CD95L on myeloid cells reduced the number of neutrophils and macrophages infiltrating the injured spinal cord, reduced the death of neurons and oligodendrocytes, and improved functional recovery following spinal cord injury (Letellier *et al*., 2010). Evidence has shown that proinflammatory and pro-apoptotic cytokines, including TNF-a, IL-1 b and Fas ligand regulate cellular events (Martin-Villalba *et al*., 1999) and downregulate proinflammatory cytokines, neutralization of IL-6 and IL-1 improve functional recovery after spinal cord injury (Okada *et al*., 2004; Akuzawa *et al*., 2008). We found that the neutralization of Fas ligand reduced the infiltration of macrophage and reactive microglia along with reducing glial scar formation in twy/twy mice. The depletion of macrophages/microglia (Popovich *et al*., 1999; Mabon *et al*., 2000), reduction of myeloperoxidase activity (Hamada *et al*., 1996) and MMP-9 null mice (Goussev *et al*., 2003) result in the reduction of secondary

demyelination and axonal loss, as well as in improved functional recovery after spinal cord injury, respectively. Fleming *et al*. (2006) reports that 5 days after spinal cord injury in humans, activated microglia and macrophages were the most common inflammatory cells in the spinal cord for up to 4 months (Buss *et al*., 2007), and a year after spinal cord injury. They also found myeloperoxidase expression for up to 1–3 days and T-cells in peak numbers between 3 and 7 days post-injury, remaining in the spinal cord for as long as 10 weeks post-spinal cord injury (Popovich *et al*., 1997). In the present study, we found that activated microglia/macrophages were the predominant inflammatory cell type in all cases of CSM from 6 months to 50 years. We also observed that myeloperoxidase-positive cells and CD3-positive lymphocytes (T-cells) were seen throughout the grey and white matter in four cases of CSM from 6 months to 11 years after onset. Furthermore, we identified that Fas ligand and CD68, as well as Fas and CD68, are colocalized in the epicentre of CSM spinal cords. It is also possible that mechanical compression and ischaemia of the cervical cord segments increased the levels of Fas ligand, leading to Fas-mediated neuronal and oligodendrocytic apoptosis. Fas-induced inflammatory responses as witnessed by microglia/macrophages after the onset of CSM from 6 months to 50 years can exacerbate the Fas-mediated tissue damage by increasing inflammatory cell infiltration with consequent release of proinflammatory cytokines. In contrast to these tissue-destructive effects, microglia/macrophages and T lymphocytes also participate in the removal of injured tissue debris following spinal cord injury and in the release of protective cytokines that promote neuronal regeneration, wound healing and tissue repair (McTigue *et al.,* 1998; Herx *et al.,* 2000; Jones *et al.,* 2005). This is significant because T lymphocytes can allow for early contact of the immune system with cellular debris, removal of pathogenic agents protecting neurons from degenerative conditions (Kipnis *et al*., 2002; Schwartz and Kipnis, 2007) and secretion of various trophic factors that are important for axonal regeneration and growth (Moalem *et al*., 2000). Therefore, further knowledge of the role of inflammatory cell infiltration in pathophysiological, neurochemical and molecular mechanisms of the disease course of CSM is needed.

In conclusion, we report novel evidence showing that Fas/Fas ligand-mediated apoptosis of neurons and oligodendrocytes and inflammation contributes to the pathobiology of spinal cord degeneration and affects neuronal function and survival in CSM. Neutralization of the Fas ligand using a function-blocking antibody reduces cell death, attenuates inflammation, promotes axonal repair and enhances functional neurological outcomes in rodent models of CSM. The targeting of a death receptor pathway is a viable neuroprotective strategy to attenuate neural degeneration and optimize neurological recovery in CSM. Our findings will open the door to the possibility of complementary treatments to surgical decompression.

Acknowledgements

The authors would like to thank Miss Allyson Tighe for her valuable comments, editing and feedback.

Funding

The Krembil Chair in Neural Repair and Regeneration; the Canadian Institutes of Health Research.

References

Ackery A, Robins S, Fehlings MG. Inhibition of Fas-mediated apoptosis through administration of soluble Fas receptor improves functional outcome and reduces posttraumatic axonal degeneration after acute spinal cord injury. J Neurotrauma 2006; 23: 604–16.

Akuzawa S, Kazui T, Shi E, Yamashita K, Bashar AH, Terada H. Interleukin-1 receptor antagonist attenuates the severity of spinal cord ischemic injury in rabbits. J Vasc Surg 2008; 48: 694–700.

Badie B, Schartner J, Vorpahl J, Preston K. Interferon-gamma induces apoptosis and augments the expression of Fas and Fas ligand by microglia in vitro. Exp Neurol 2000; 162: 290–6.

Becher B, Barker PA, Owens T, Antel JP. CD95-CD95L: can the brain learn from the immune system? Trends Neurosci 1998; 21: 114–7.

Bohlman HH, Emery SE. The pathophysiology of cervical spondylosis and myelopathy. Spine 1988; 13: 843–6.

Buss A, Pech K, Kakulas BA, Martin D, Schoenen J, Noth J, et al. Matrix metalloproteinases and their inhibitors in human traumatic spinal cord injury. BMC Neurol 2007; 7: 17.

Carter RJ, Lione LA, Humby T, Mangiarini L, Mahal A, Bates GP, et al. Characterization of progressive motor deficits in mice transgenic for the human Huntington's disease mutation. J Neurosci 1999; 19: 3248–57.

Casha S, Yu WR, Fehlings MG. Oligodendroglial apoptosis occurs along degenerating axons and is associated with FAS and p75 expression following spinal cord injury in the rat. Neuroscience 2001; 103: 203–18.

Casha S, Yu WR, Fehlings MG. FAS deficiency reduces apoptosis, spares axons and improves function after spinal cord injury. Exp Neurol 2005; 196: 390–400.

Choi K, Benveniste EN, Choi C. Induction of intercellular adhesion molecule-1 by Fas ligation: proinflammatory roles of Fas in human astroglioma cells. Neurosci Lett 2003; 352: 21–4.

Cregan SP, Fortin A, MacLaurin JG, Callaghan SM, Cecconi F, Yu SW, et al. Apoptosis-inducing factor is involved in the regulation of caspase-independent neuronal cell death. J Cell Biol 2002; 158: 507–17.

Crowe MJ, Bresnahan JC, Shuman SL, Masters JN, Beattie MS. Apoptosis and delayed degeneration after spinal cord injury in rats and monkeys. Nat Med 1997; 3: 73–6.

de Medinaceli L, Freed WJ, Wyatt RJ. An index of the functional condition of rat sciatic nerve based on measurements made from walking tracks. Exp Neurol 1982; 77: 634–43.

Demjen D, Klussmann S, Kleber S, Zuliani C, Stieltjes B, Metzger C, et al. Neutralization of CD95 ligand promotes regeneration and functional recovery after spinal cord injury. Nat Med 2004; 10: 389–95.

Desbarats J, Birge RB, Mimouni-Rongy M, Weinstein DE, Palerme JS, Newell MK. Fas engagement induces neurite growth through ERK activation and p35 upregulation. Nat Cell Biol 2003; 5: 118–25.

Emery E, Aldana P, Bunge MB, Puckett W, Srinivasan A, Keane RW, et al. Apoptosis after traumatic human spinal cord injury. J Neurosurg 1998; 89: 911–20.

Fehlings MG, Skaf G. A review of the pathophysiology of cervical spondylotic myelopathy with insights for potential novel mechanisms drawn from traumatic spinal cord injury. Spine 1998; 23: 2730–7.

Felderhoff-Mueser U, Taylor DL, Greenwood K, Kozma M, Stibenz D, Joashi UC, et al. Fas/CD95/APO-1 can function as a death receptor for neuronal cells in vitro and in vivo and is upregulated following cerebral hypoxic-ischemic injury to the developing rat brain. Brain Pathol 2000; 10: 17–29.

Fleming JC, Norenberg MD, Ramsay DA, Dekaban GA, Marcillo AE, Saenz AD, et al. The cellular inflammatory response in human spinal cords after injury. Brain 2006; 129: 3249–69.

Giulian D, Corpuz M. Microglial secretion products and their impact on the nervous system. Adv Neurol 1993; 59: 315–20.

Goussev S, Hsu JY, Lin Y, Tjoa T, Maida N, Werb Z, et al. Differential temporal expression of matrix metalloproteinases after spinal cord injury: relationship to revascularization and wound healing. J Neurosurg 2003; 99: 188–97.

Hamada Y, Ikata T, Katoh S, Nakauchi K, Niwa M, Kawai Y, et al. Involvement of an intercellular adhesion molecule 1-dependent pathway in the pathogenesis of secondary changes after spinal cord injury in rats. J Neurochem 1996; 66: 1525–31.

Hausmann ON. Post-traumatic inflammation following spinal cord injury. Spinal Cord 2003; 41: 369–78.

Herx LM, Rivest S, Yong VW. Central nervous system-initiated inflammation and neurotrophism in trauma: IL-1 beta is required for the production of ciliary neurotrophic factor. J Immunol 2000; 165: 2232–9.

Jones TB, Hart RP, Popovich PG. Molecular control of physiological and pathological T-cell recruitment after mouse spinal cord injury. J Neurosci 2005; 25: 6576–83.

Keane RW, Kraydieh S, Lotocki G, Bethea JR, Krajewski S, Reed JC, et al. Apoptotic and anti-apoptotic mechanisms following spinal cord injury. J Neuropathol Exp Neurol 2001; 60: 422–9.

Kipnis J, Mizrahi T, Hauben E, Shaked I, Shevach E, Schwartz M. Neuroprotective autoimmunity: naturally occurring CD4 + CD25 + regulatory T cells suppress the ability to withstand injury to the central nervous system. Proc Natl Acad Sci USA 2002; 99: 15620–5.

Letellier E, Kumar S, Sancho-Martinez I, Krauth S, Funke-Kaiser A, Laudenklos S, et al. CD95-ligand on peripheral myeloid cells activates Syk kinase to trigger their recruitment to the inflammatory site. Immunity 2010; 32: 240–52.

Li GL, Brodin G, Farooque M, Funa K, Holtz A, Wang WL, et al. Apoptosis and expression of Bcl-2 after compression trauma to rat spinal cord. J Neuropathol Exp Neurol 1996; 55: 280–9.

Li GL, Farooque M, Holtz A, Olsson Y. Apoptosis of oligodendrocytes occurs for long distances away from the primary injury after compression trauma to rat spinal cord. Acta Neuropathol 1999; 98: 473–80.

Lou J, Lenke LG, Ludwig FJ, O'Brian MF. Apoptosis as a mechanism of neuronal cell death following acute experimental spinal cord injury. Spinal Cord 1998; 36: 683–90.

Mabon PJ, Weaver LC, Dekaban GA. Inhibition of monocyte/macrophage migration to a spinal cord injury site by an antibody to the integrin alphaD: a potential new anti-inflammatory treatment. Exp Neurol 2000; 166: 52–64.

Martin-Villalba A, Hahne M, Kleber S, Vogel J, Falk W, Schenkel J, et al. Therapeutic neutralization of CD95-ligand and TNF attenuates brain damage in stroke. Cell Death Differ 2001; 8: 679–86.

Martin-Villalba A, Herr I, Jeremias I, Hahne M, Brandt R, Vogel J, et al. CD95 ligand (Fas-L/APO-1 L) and tumor necrosis factor-related apoptosis-inducing ligand mediate ischemia-induced apoptosis in neurons. J Neurosci 1999; 19: 3809–17.

McCormack BM, Weinstein PR. Cervical spondylosis. An update. West J Med 1996; 165: 43–51.

McTigue DM, Tani M, Krivacic K, Chernosky A, Kelner GS, Maciejewski D, et al. Selective chemokine mRNA accumulation in the rat spinal cord after contusion injury. J Neurosci Res 1998; 53: 368–76.

Moalem G, Gdalyahu A, Shani Y, Otten U, Lazarovici P, Cohen IR, et al. Production of neurotrophins by activated T cells: implications for neuroprotective autoimmunity. J Autoimmun 2000; 15: 331–45.

Nakamura I, Ikegawa S, Okawa A, Okuda S, Koshizuka Y, Kawaguchi H, et al. Association of the human NPPS gene with ossification of the posterior longitudinal ligament of the spine (OPLL). Hum Genet 1999; 104: 492–7.

O'Connell J, Houston A, Bennett MW, O'Sullivan GC, Shanahan F. Immune privilege or inflammation? Insights into the Fas ligand enigma. Nat Med 2001; 7: 271–4.

Ohwada T, Ohkouchi T, Yamamoto T, Ono K. [Symptoms and pathological anatomy of the degenerative cervical spine]. Orthopade 1996; 25: 496–504.

Okada S, Nakamura M, Mikami Y, Shimazaki T, Mihara M, Ohsugi Y, et al. Blockade of interleukin-6 receptor suppresses reactive astrogliosis and ameliorates functional recovery in experimental spinal cord injury. J Neurosci Res 2004; 76: 265–76.

Pallier PN, Drew CJ, Morton AJ. The detection and measurement of locomotor deficits in a transgenic mouse model of Huntington's disease are task- and protocol-dependent: influence of non-motor factors on locomotor function. Brain Res Bull 2009; 78: 347–55.

Popovich PG, Guan Z, Wei P, Huitinga I, van Rooijen N, Stokes BT. Depletion of hematogenous macrophages promotes partial hindlimb recovery and neuroanatomical repair after experimental spinal cord injury. Exp Neurol 1999; 158: 351–65.

Popovich PG, Wei P, Stokes BT. Cellular inflammatory response after spinal cord injury in Sprague-Dawley and Lewis rats. J Comp Neurol 1997; 377: 443–64.

Pouly S, Becher B, Blain M, Antel JP. Interferon-gamma modulates human oligodendrocyte susceptibility to Fas-mediated apoptosis. J Neuropathol Exp Neurol 2000; 59: 280–6.

Schwartz M, Kipnis J. Model of acute injury to study neuroprotection. Methods Mol Biol 2007; 399: 41–53.

Spanaus KS, Schlapbach R, Fontana A. TNF-alpha and IFN-gamma render microglia sensitive to Fas ligand-induced apoptosis by induction of Fas expression and down-regulation of Bcl-2 and Bcl-xL. Eur J Immunol 1998; 28: 4398–408.

Springer JE, Azbill RD, Knapp PE. Activation of the caspase-3 apoptotic cascade in traumatic spinal cord injury. Nat Med 1999; 5: 943–6.

Swagerty DL Jr. Cervical spondylotic myelopathy: a cause of gait disturbance and falls in the elderly. Kans Med 1994; 95: 226–7, 229.

Uchida K, Baba H, Maezawa Y, Furukawa S, Furusawa N, Imura S. Histological investigation of spinal cord lesions in the spinal hyperostotic mouse (twy/twy): morphological changes in anterior horn cells and immunoreactivity to neurotropic factors. J Neurol 1998; 245: 781–93.

Yamaura I, Yone K, Nakahara S, Nagamine T, Baba H, Uchida K, et al. Mechanism of destructive pathologic changes in the spinal cord under chronic mechanical compression. Spine 2002; 27: 21–6.

Yoshino O, Matsuno H, Nakamura H, Yudoh K, Abe Y, Sawai T, et al. The role of Fas-mediated apoptosis after traumatic spinal cord injury. Spine 2004; 29: 1394–404.

Yu WR, Baptiste DC, Liu T, Odrobina E, Stanisz GJ, Fehlings MG. Molecular mechanisms of spinal cord dysfunction and cell death in the spinal hyperostotic mouse: implications for the pathophysiology of human cervical spondylotic myelopathy. Neurobiol Dis 2009a; 33: 149–63.

Yu WR, Liu T, Fehlings TK, Fehlings MG. Involvement of mitochondrial signaling pathways in the mechanism of Fas-mediated apoptosis after spinal cord injury. Eur J Neurosci 2009b; 29: 114–31.

Zurita M, Vaquero J, Zurita I. Presence and significance of CD-95 (Fas/APO1) expression after spinal cord injury. J Neurosurg 2001; 94: 257–64.